

## Análise por espectroscopia no infravermelho das camadas de fosfato de zinco e de zinco modificado com níquel e manganês em aço eletrolgalvanizado

*Infrared-spectroscopy analysis of zinc phosphate and nickel and manganese modified zinc phosphate coatings on electrogalvanized steel*

### **Kirlene Salgado Fernandes**

Industrial Chemist, M.Sc.,  
Research & Development Center,  
Usiminas Industry, Brazil  
[kirlene@uol.com.br](mailto:kirlene@uol.com.br)

### **Evandro de Azevedo Alvarenga**

Chemical Engineer, M.Sc.,  
Research & Development Center,  
Usiminas Industry, Brazil  
[ealvarenga@usiminas.com.br](mailto:ealvarenga@usiminas.com.br)

### **Paulo Roberto Gomes Brandão**

Mining Engineering, M.Sc., PhD,  
Federal University of Minas Gerais,  
Belo Horizonte, Brazil  
[pbrandao@demin.ufmg.br](mailto:pbrandao@demin.ufmg.br)

### **Vanessa de Freitas Cunha Lins**

Chemical Engineer, Sc.Dr., Corrosion  
and Surface Engineering Laboratory,  
Federal University of Minas Gerais,  
Belo Horizonte, Brazil  
[vanessa.lins@terra.com.br](mailto:vanessa.lins@terra.com.br)

### **Resumo**

As camadas de fosfato do tipo hopeíta, nas quais o zinco é parcialmente substituído por outros metais, como manganês e níquel, são de grande interesse para a indústria automotiva e de eletrodomésticos. Essas indústrias utilizam aços galvanizados, fosfatizados e pintados com eletropintura cataforética. Os fosfatos de zinco modificados com manganês e níquel são isomorfos com a hopeíta, e de difícil identificação usando-se a técnica de difração de raios X. Nesse trabalho, as camadas de conversão de fosfato foram identificadas usando-se a espectroscopia no infravermelho por transformada de Fourier (FTIR).

**Palavras-chave:** Superfícies, fosfato de zinco, recobrimentos, espectroscopia no infra-vermelho

### **Abstract**

*Hopeite-type phosphate coatings in which zinc is partially replaced by other metals like manganese and nickel are of great interest for the automotive and home appliance industries. Such industries use phosphate conversion coatings on galvanized steels in association with cathodic electropainting. Zinc phosphates modified with manganese and nickel are isomorphic with the hopeite, and the phase identification using X-ray diffraction is difficult. In this paper, the phosphate coatings are identified using the Fourier transform infrared spectroscopy (FTIR).*

**Keywords:** Surfaces, zinc phosphate, coatings, infrared spectroscopy.

### **1. Introduction**

The phosphating process is widely used by the industry as a pre-treatment of metallic surfaces before painting, promoting the paint adherence and protecting the substrate against corrosion.

Zinc phosphate coatings on steel con-

sist mainly of crystalline  $\alpha$ - hopeite, orthorhombic  $\alpha$ -  $[\text{Zn}_3(\text{PO}_4)_2 \cdot 4\text{H}_2\text{O}]$  and crystalline phosphophyllite  $[\text{Zn}_2\text{Fe}(\text{PO}_4)_2 \cdot 4\text{H}_2\text{O}]$  (Pawlig & Trettin, 1999). The relative amount of these two phases is a widely used parameter for the evaluation of the

corrosion resistance of the steel/phosphate/paint system (Yoshihara & Okita, 1983). The corrosion and adhesion behaviors of these phosphate layers are improved when the phosphophyllite-hopeite ratio increases (Fedrizzi et al., 2001).

However, when the metallic substrates are zinc-coated steels only hopeite is formed. Phosphophyllite has been shown to be more resistant than hopeite in aqueous media (Narayanan & Subbaiyan, 1993). Since the hopeite has a low weather corrosion resistance the painting scheme is impaired as the corrosive process proceeds,

## 2. Experimental

The electrogalvanized steel sheet was produced by Usiminas Steel Works (Alvarenga et al., 1994) and the phosphating of the samples was performed at the laboratory of Henkel Surface Technologies Brasil Ltda., by immersion in phosphating baths with the compositions presented in Table 1.

In the phosphating process the samples were degreased with a 3 wt.% solution of the product Parco Cleaner 1522 AV at 333 K, and rinsed with water (Fernandes, 2002). The samples were then immersed in a bath containing 1 g/L of the titanium-based refiner Fixodine 18 for 30 s at the temperature of 333 K. Refiner is used to prepare the metallic surface for the nucleation and growth of the phosphate crystals. In the next step the samples were immersed in the phosphating solution for 1 minute at the temperature of 333 K and rinsed with running water and dried at 373 K for 2 minutes. This procedure was used

due to the cathodic character of the corrosion front.

Secondary elements such as Ni<sup>2+</sup> and Mn<sup>2+</sup> are used to increase the zinc phosphate alkaline stability. Fedrizzi et al. (2001) reported that electrochemical and cathodic delamination tests showed that zinc phosphate treatments, and in particular phosphatization baths containing manganese, greatly improve the metal - paint adhesion under the very stressing condition typical of the water heaters.

However, the phosphates containing manganese and nickel in their structure

are isomorphous in relation to hopeite, and the phase identification using X-ray diffraction is difficult. The development of a methodology for the identification of phases and compounds, whether crystalline or not, present in the phosphate layer of zinc-coated steels is very important for the industries whose products are phosphated and painted.

In the present work, Fourier transform infrared spectroscopy (FTIR) was used for the analysis of phosphate layers produced from phosphating solutions with different chemical compositions.

for each of the phosphating baths shown in Table 1.

The samples were weighed in an analytical balance with a precision of 0.1 mg. The phosphate layer was removed by immersing each sample in a solution of CrO<sub>3</sub> (0.5% wt./vol. at 343 K) for 5 minutes. The samples were then rinsed with distilled water, dried and weighed again.

The solution used for the removal of the phosphate coating on each sample was calibrated and then analyzed by atomic absorption spectroscopy for the determination of the elements present in the coating. The equipment used was an Inductive Coupled Plasma Spectrometer -Spectroflame Modula.

The morphology of the phosphate coating was characterized by scanning electron microscopy (SEM) using a Stereoscan 360/Cambridge microscope.

The analyses by Fourier transform infrared spectroscopy (FTIR) were performed with a Perkin-Elmer Paragon-

Spectrum 1000 FTIR Spectrometer, using the specular reflectance accessory with a fixed angle of incidence of 16°, spectral resolution of 2 cm<sup>-1</sup> and the average of 32 single scans. The result obtained using this technique is the same as that obtained using transmission in a film self-supported film with double thickness, and the results are shown as transmission values.

The phosphated samples were heat-treated and analyzed again using the same Fourier transform infrared spectroscopy technique. The objective of the heat treatment was to verify the changes, which could take place in the coatings, such as partial or total dehydration, as well as to aid the identification of the phases present in the phosphate coating. The heat treatment was performed in a drying and sterilizing oven Fanem model 920SE - Mechanical Circulation, during 1 hour, at 393 K for samples E-F2 and E-F4, 413 K for samples E-F1 and E-F3 and 453 K for the sample E-F5.

Identification of the samples	Type of coating formed	Chemical composition of the bath (g/L)			Acidity (mL NaOH 0,1N)	
		Zn	Mn	Ni	Free	Total
E-F1	tri-cation	1.18	0.73	0.68	0.50	18.0
E-F2	pure hopeite	1.23	-	-	0.50	17.9
E-F3	Mn-modified hopeite	1.15	0.80	-	0.60	17.9
E-F4	Ni-modified hopeite (low content)	1.16	-	0.43	0.50	17.8
E-F5	Ni-modified hopeite (high content)	1.16	-	0.86	0.60	17.9

Table 1  
Chemical composition of the baths used in the phosphating of electrogalvanized steels.

## 3. Results and discussion

The results in Table 2 show that the mass of the phosphate coating varied according to the composition of the phosphating bath. Sample E-F1, a tricationic phosphate layer on electrogalvanized steel,

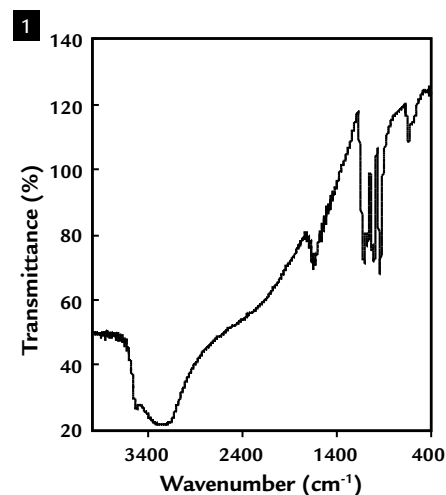
showed the highest phosphate coating mass while the lowest mass corresponded to the Zn/Mn phosphate layer on zinc coated steel. Manganese has a lower molecular mass than zinc and nickel, the

other elements that constitute the phosphate layer. This variation was attributed to the chemical reactivity of each phosphating bath. The structure of inorganic phosphate coatings depends on their film

Table 2  
Mass and chemical composition  
of the phosphate coating applied  
on the electrogalvanized steels.

Sample	Phosphate Coating				
	Mass (g/m <sup>2</sup> )	Chemical Composition (wt %)			
		Zn	P	Mn	Ni
E-F1	3.2	42.2	9.4	3.9	1.4
E-F2	2.1	54.6	12.7	< 0.1	< 0.1
E-F3	1.7	37.2	9.6	4.0	< 0.1
E-F4	2.9	47.0	8.3	< 0.1	1.3
E-F5	2.1	64.8	12.9	< 0.1	2.7

Figure 1  
Infrared spectrum of  
the phosphate coating of  
sample E-F2 (pure hopeite).



weight (Weng et al., 1996). Middle-weight (1.4 -7.5 g/m<sup>2</sup>) as well as heavy-weight (7.5 -30 g/m<sup>2</sup>) phosphate film demonstrates a crystal structure (Weng et al, 1996). The phosphate coatings studied can be classified as middle-weight according to Table 2.

The phosphate crystals were fine, compact and had the shape of platelets, uniformly covering the surface of the samples. No significant differences were observed between the phosphate coatings for the samples investigated. Fedrizi et al. (2001) related that the main difference between the zinc phosphate and the tri-cation phosphate appears to be the phosphate crystal size, which is much smaller in the case of the tri-cation phosphate process.

Figure 1 shows an infrared spectrum representative of the phosphate coatings investigated in this work, while Table 3 shows the band positions in the infrared

spectrum of each phosphate coating.

According to the results given in Table 3 the phosphate coatings show several bands with strong absorption between 1200 cm<sup>-1</sup> and 900 cm<sup>-1</sup> in the spectrum. The spectra show characteristic absorptions due to the PO<sub>4</sub><sup>3-</sup> group ( $\nu_1$ : 929 cm<sup>-1</sup>,  $\nu_3$ : 1105, 1066, 1026, and 1000 cm<sup>-1</sup>,  $\nu_4$ : 635 cm<sup>-1</sup>). These results confirm the observations by Molt et al. (1994) and Pawlig and Trettin (1999).

In addition, water bending (1639 cm<sup>-1</sup>) and OH stretching (3546 cm<sup>-1</sup> and a broad band centered at 3300-3400 cm<sup>-1</sup>) vibrations can be observed (Figure 1 and Table 3). Their positions are consistent with the presence of a hydrogen-bonding network within the crystal lattice. However, the sharp band at 3546 cm<sup>-1</sup> indicates that some OH groups do not participate in hydrogen bonding. Frost (2004) identified four infrared bands of the hydroxyl

stretching region of hopeite, which are at 3542, 3473, 3338, and 3149 cm<sup>-1</sup>. Pawling et al (2001) reported the infrared spectrum of hopeite and its deuterium-analogs. They reported infrared bands at 3537, 3410, 3263, and 3181 cm<sup>-1</sup>. The structure of hopeite consists of ZnO<sub>2</sub>(H<sub>2</sub>O)<sub>4</sub> octahedra, ZnO<sub>4</sub> tetrahedra, and PO<sub>4</sub> tetrahedra, none of which are regular, these polyhedra share corners and edges (Whitaker, 1975). It is likely that the two water molecules are non-equivalent, thus giving rise to in-phase and out-of-phase behavior. Hence, two infrared bands would be expected. In this work, two infrared bands of the hydroxyl stretching region of hopeite are observed, at 3510 and 3265 cm<sup>-1</sup> (Table 3).

The numerous bands in the phosphate region can be explained by the low C<sub>1</sub> site symmetry of the phosphate ion in the hopeite structure. Hopeite (EF-2) showed three intense bands: a single band

Table 3  
Position of bands in the  
infrared spectra of the phosphate  
coatings applied on the  
electrogalvanized steel.

Sample	Position of Bands (cm <sup>-1</sup> )				
	$\nu$ (OH)	$\nu$ (H <sub>2</sub> O)	$\delta$ (H <sub>2</sub> O)	$\nu$ (PO <sub>4</sub> <sup>-3</sup> )	$\delta$ (PO <sub>4</sub> <sup>-3</sup> )
E-F1	3541	3276	1636	1101/1066 1018/994 927	629
E-F2	3510	3265	1628	1104/1067 1019/1000 935	631
E-F3	3535	3264	1627	1106/1068 1021/1001 938	635
E-F4	3528	3277	1627	1102/1066 1017/994 929	628
E-F5	3528	3275	1636	1101/1065 1017/994 929	628

at 935  $\text{cm}^{-1}$  and two doublets at 1019  $\text{cm}^{-1}/1000 \text{ cm}^{-1}$  and 1104  $\text{cm}^{-1}/1067 \text{ cm}^{-1}$ , Table 3 and Figure 2. The bands at 1019, 1000, 1104 and 1067  $\text{cm}^{-1}$  are assigned to the  $\nu_3 \text{ PO}_4$  antisymmetric stretching modes (Frost, 2004). The band at 935  $\text{cm}^{-1}$  is ascribed to the  $\nu_1$  symmetric stretching modes. Frost (2004) identified bands at 1137, 1096, 1059, 1019, 995  $\text{cm}^{-1}$ , which are assigned to the  $\nu_3 \text{ PO}_4$  antisymmetric stretching modes (Frost, 2004), and bands at 945 and 922  $\text{cm}^{-1}$  ascribed to the  $\nu_1$  symmetric stretching modes, in the hopeite infrared spectrum. Molt et al. (1994) identified only one doublet for pure hopeite at 1099  $\text{cm}^{-1}/1070 \text{ cm}^{-1}$  and also reported an additional band at 1020  $\text{cm}^{-1}$  for the compounds derived from the hopeite with manganese and/or nickel, which has not been observed in the present work, according to the results shown in Table 3.

Table 4 shows the position of the bands in the infrared spectra of phosphate coatings after heat treatment.

As can be seen in Table 4 the partial dehydration of the phosphate coatings start at 393 K for the samples E-F2 and E-F4.

The (OH) vibration peak, around 3500  $\text{cm}^{-1}$ , disappears at 393 K for the hopeite (sample E-F2). Pawlig and Trettin (1999) reported that when a heating rate of 5 or 10 K/min was used, the dehydration of  $\alpha$ -hopeite was accompanied by three endothermic effects. The onset temperatures were 374, 411, and 542 K for a heating rate of 10 k/min and 363, 410, and 535 K for a heating rate of 5 K/min. Pawlig and Trettin (1999) observed that the first and second endothermic peaks in the differential thermal analysis curve can be assigned to the group of weaker bonded or free OH ( $\text{Zn}^{2+} - \text{OH}_2 - \text{OH}_2$ ), giving rise to higher stretching frequencies (3292 - 3531  $\text{cm}^{-1}$ ). The bonds in the group of weaker bonded OH are weaker for the  $\text{Zn}^{2+}$  cations, more electronegative than  $\text{Mn}^{2+}$  and  $\text{Ni}^{2+}$ . This hypothesis is according to the obtained

result; the partial dehydration of the zinc phosphate coatings and the low-nickel zinc phosphate coatings started at a lowest temperature (393 K).

The  $\nu(\text{OH})$  vibration peak, around 3500  $\text{cm}^{-1}$ , disappears at 413 K for tri-cation phosphate and manganese-modified zinc phosphate, and at 453 K for nickel modified zinc phosphate. The bonds in the group of weaker bonded OH are stronger for the cations  $\text{Mn}^{2+}$  and  $\text{Ni}^{2+}$ , more electropositive than zinc cations.

Table 4 also shows some alterations after heat treatment in the  $\nu(\text{PO}_4^{3-})$  vibration region in the range between 1200  $\text{cm}^{-1}$  and 900  $\text{cm}^{-1}$  in relation to the data in Table 3. It is thus possible to identify the phosphate coating of sample E-F1, heat treated at 413 K, by observing the absence of both doublets which became single peaks. For the samples E-F3 and E-F5, after heat treating at 413 K and at 393 K, the peaks at 1068  $\text{cm}^{-1}/1001 \text{ cm}^{-1}$  and 994  $\text{cm}^{-1}$  disappeared.

Sample	Position of Bands ( $\text{cm}^{-1}$ )				
	$\nu(\text{OH})$	$\nu(\text{H}_2\text{O})$	$\delta(\text{H}_2\text{O})$	$\nu(\text{PO}_4^{3-})$	$\delta(\text{PO}_4^{3-})$
E-F1 (413 K)	-	3314	1627	1075 1005 941	619 459
E-F2 (393 K)	-	3274	1627	1105/1066 1004 938	631
E-F3 (413 K)	-	3210	1624	1106 1018 951	639
E-F4 (393 K)	3527	3262	1636	1101/1066 994/1014 929	629 576
E-F5 (453 K)	-	3392	1636	1118/1076 1021 934	617

Table 4  
Band positions of the infrared spectra for the phosphate coatings applied on the electrogalvanized steel after heat treatment.

#### 4. Conclusions

The partial dehydration of the zinc phosphate coatings and the low-nickel zinc phosphate coatings started at a lowest temperature (393 K).

The  $\nu(\text{OH})$  vibration peak, around

3500  $\text{cm}^{-1}$ , disappears at 413 K for the manganese and nickel modified hopeite and the manganese-modified zinc phosphate, and at 453 K for the high-nickel modified zinc phosphate.

Alterations in the spectra of phosphate coatings on steel after heat treatment in the  $\nu(\text{PO}_4^{3-})$  vibration region were identified.

It is possible to identify the man-

ganese and nickel modified hopeite, heat treated at 413 K, by observing the absence of both doublets at 1101/1066 and

1018/994  $\text{cm}^{-1}$ , which became single peaks.

For the manganese modified hopeite and high-nickel modified hopeite, after

heat treating at 413 K and at 393 K, the peaks at 1068  $\text{cm}^{-1}$ /1001  $\text{cm}^{-1}$  and 994  $\text{cm}^{-1}$  disappeared.

## 5. Acknowledgements

This work was supported by the Research Support Foundation of Minas

Gerais, FAPEMIG, Henkel Surface Technologies Brasil Ltda, and Usiminas

Industry.

## 6. References

- ALVARENGA, E.A., SOUSA, J.G., OLIVEIRA, G.A, MACHADO, G.O. Implantação da linha de galvanização eletrolítica da USIMINAS. *Metalurgia & Materiais*, v.50, n. 425, p.74-79, 1994.
- FEDRIZI, L., DEFLORIAN, F., ROSSI, S., FAMBRI, L., BONORA, P.L. Study of the corrosion behaviour of phosphatized and painted industrial water heaters. *Progress in Organic Coatings*, v. 42, p.65, 2001.
- FERNANDES, K.S. *Characterization of the phosphate coating in galvanized steels by Fourier Transform infrared spectroscopy*. Belo Horizonte, Brazil: Federal University of Minas Gerais, March/2002. (M. Sc. Thesis).
- FROST, R.L. An infrared and Raman spectroscopic study of natural zinc phosphates. *Spectrochimica Acta Part A*, v. 60, p.1439-1445, 2004.
- MOLT, K., POHL, M., SEIDEL, R., MAYER, B. IR-Spectroscopic investigations on phosphated galvanized steel. *Microchimica Acta*, v. 116, p.101, 1994.
- NARAYANAN, T.S.N.S., SUBBAIYAN, M. Effect of surfactants on the porosity and corrosion resistance of zinc-phosphated steel. *Met. Finish*, v. 91, p.51, 1993.
- PAWLIG, O., TRETTIN, R. Synthesis and characterization of  $\alpha$ -hopeite,  $\text{Zn}(\text{PO}_4)\cdot 4\text{H}_2\text{O}$ . *Materials Research Bulletin*, v. 34, n. 12/13, p.1959, 1999.
- PAWLIG, O., SCHELLENCHLAGER, V., LUTZ, H.D., TRETTIN, R. Vibrational analysis of iron and zinc phosphate conversion coating constituents. *Spectrochim Acta Part A : Mol. Biomol. Spectrosc.*, v. 57 A, p. 581, 2001.
- WENG, D., JOKIEL, P., UEBLEIS, A, BOEHNI, H. Corrosion and protection characteristics of zinc and manganese phosphate coatings. *Surface and Coatings Technology*, v. 88, p.147-156, 1997.
- WHITAKER, A. The crystal structure of hopeite,  $\text{Zn}_3(\text{PO}_4)_2\cdot 4\text{H}_2\text{O}$ . *Acta Crystallographica Section B. Structural Crystallography and Crystal Chemistry*, v. 34, p. 2385-2386, 1978.
11. YOSHIHARA, T., OKITA, H. Phosphate coating techniques for car bodies. *Transactions ISIJ*, v.23, n. 11, p. 984-993, 1983.

---

Artigo recebido em 14 de dezembro de 2006 . Aprovado em 11 de outubro de 2010.